

Miniature diamond anvil pressure cell for single crystal x-ray diffraction studies

Leo Merrill and William A. Bassett

Citation: [Review of Scientific Instruments](#) **45**, 290 (1974); doi: 10.1063/1.1686607

View online: <http://dx.doi.org/10.1063/1.1686607>

View Table of Contents: <http://aip.scitation.org/toc/rsi/45/2>

Published by the [American Institute of Physics](#)

Articles you may be interested in

[Ultrahigh pressure diamond-anvil cell and several semiconductor phase transition pressures in relation to the fixed point pressure scale](#)

[Review of Scientific Instruments](#) **46**, 973 (2008); 10.1063/1.1134381

[New diamond cell for single-crystal x-ray diffraction](#)

[Review of Scientific Instruments](#) **77**, 115103 (2006); 10.1063/1.2372734

[Elements of X-Ray Diffraction](#)

[American Journal of Physics](#) **25**, 394 (2005); 10.1119/1.1934486

[An Optical Fluorescence System for Quantitative Pressure Measurement in the Diamond-Anvil Cell](#)

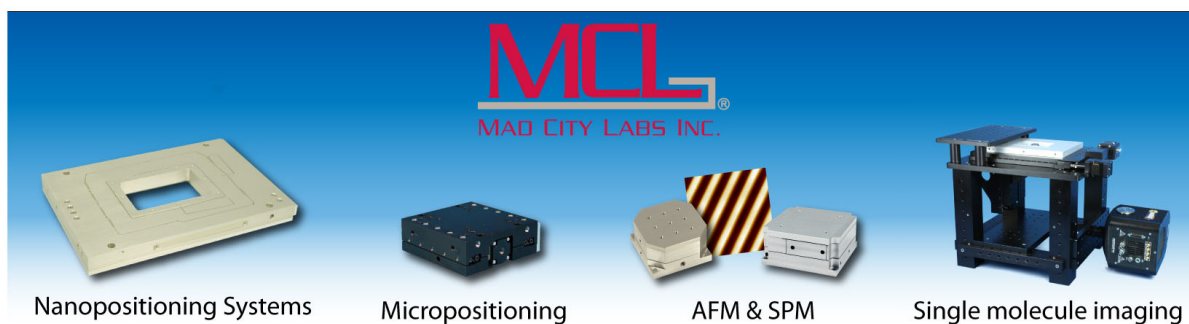
[Review of Scientific Instruments](#) **44**, 1 (2003); 10.1063/1.1685943

[Hydrostatic limits in liquids and solids to 100 kbar](#)

[Journal of Applied Physics](#) **44**, 5377 (2003); 10.1063/1.1662159

[New Device for Obtaining X-Ray Diffraction Patterns from Substances Exposed to High Pressure](#)

[Review of Scientific Instruments](#) **30**, 1016 (2004); 10.1063/1.1716408



Miniature diamond anvil pressure cell for single crystal x-ray diffraction studies

Leo Merrill* and William A. Bassett

Department of Geological Sciences, University of Rochester, Rochester, New York 14627

(Received 2 July 1973; and in final form, 10 September 1973)

A new miniature gasketed diamond anvil high pressure cell has been constructed to perform optical and x-ray diffraction studies on single crystals under hydrostatic pressure. For x-ray studies the cell is mounted on a standard goniometer head which may be attached to either a standard precession camera or single crystal orienter taking advantage of counting methods. The pressure cell has been used successfully in the study of the two high pressure phases of calcium carbonate, $\text{CaCO}_3(\text{II})$ and $\text{CaCO}_3(\text{III})$.

INTRODUCTION

In the last few years, the diamond anvil pressure cell has found extensive application in a wide variety of high pressure experiments. A few of these include (i) studies of high pressure phases using x-ray diffraction powder methods,¹ (ii) compressibility studies using both powder² and single crystal³ x-ray diffraction methods, (iii) x-ray diffraction studies of single crystal phases encapsulated in gasketed diamond anvil cells,^{4,5} (iv) synthesis of diamond,⁶ (v) melting curve of iron, and optical studies which include (vi) measurement of refractive index, (vii) Raman and (viii) infrared spectroscopy.⁷ One of the more specialized techniques involving diamond anvils has been the study of single crystal phases at high pressure.

The method of encapsulating liquids within a small diameter hole of metal foil placed between the flat parallel faces of diamonds was developed by Van Valkenburg.⁸ With this technique, it was possible to apply pressure to liquids due to the compressible nature of the metal gasket. It was then demonstrated that it was possible to grow single crystal phases from liquids under pressure or to subject a crystal immersed in an appropriate liquid to a purely hydrostatic pressure. This development led initially to the study of optical properties of liquids and solids under pressure,⁹ and finally to the development of a pressure cell designed to study single crystal phases by x-ray diffraction.¹⁰ This work was pioneered by the National Bureau of Standards group employing a pressure cell constructed of beryllium and mounted on a precession camera for data collection. The pressure is generated in this cell by a lever arm actuated by a spring loading mechanism.⁴ A diamond anvil pressure cell designed for use with a standard precession camera was developed by Fourme.¹¹ In this instrument the pressure is generated by means of a pneumatic device and can be controlled very accurately.

The main problem encountered in making an x-ray analysis of a single crystal encapsulated in a gasketed diamond anvil pressure cell is the limited region in reciprocal space that is available for examination. The NBS group solved this problem in part by constructing the entire press out of beryllium.⁴ However, since the gasket is usually made out of Inconel or some other x-ray opaque metal, a significant region of reciprocal space is still inaccessible. The NBS cell has been used only with the precession method and has not been adapted for counting techniques due to its inconvenient

shape and size. Furthermore, the need for specialized diffraction equipment and the relatively high cost involved has discouraged the general use of this technique by others.

There are some disadvantages of having to rely entirely on precession data in view of the limitations imposed by the pressure cell. Data collection in the precession method requires layers of reciprocal lattice planes for interpretation. Due to the constraints in possible orientations of the crystal, only a restricted number of these reciprocal lattice planes can be located. In studying crystals of the $\text{CaCO}_3(\text{II})$ phase which had been ground and polished perpendicular to the original calcite *c*-axis, some difficulty was encountered in resolving to which level some of the upper level spots belonged. This was due in part to the closely spaced reciprocal lattice planes and also to the difficulty encountered in aligning the sample as a result of the presence of the many weak reflections whose intensities were further diminished by the high background scattering from the diamonds. With this same sample, the use of the single crystal orienter overcame this problem since it has the advantage of point-

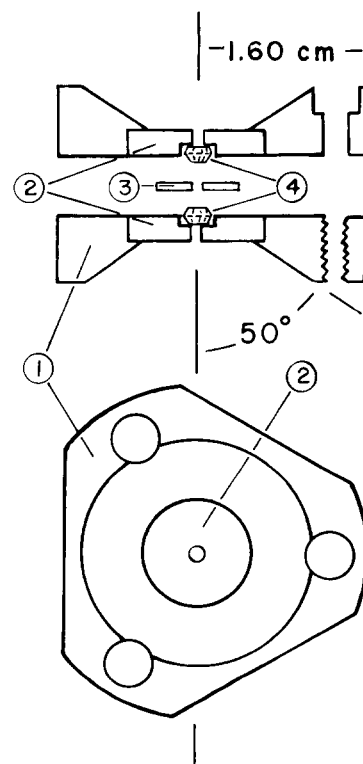
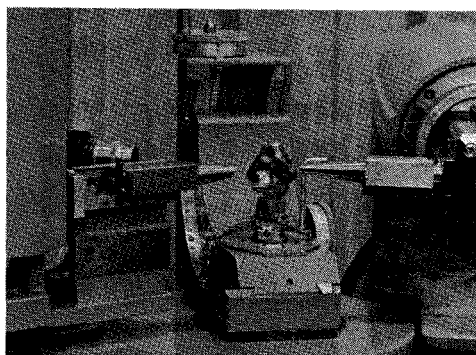
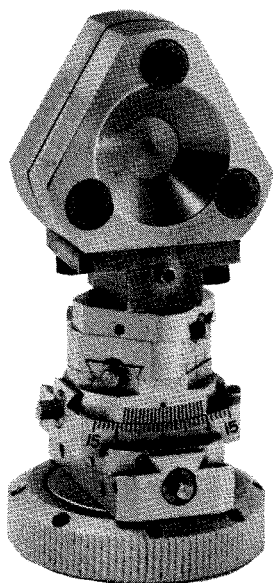


FIG. 1. Diagram of miniature gasketed diamond anvil pressure cell. (1)—Stainless steel platens; (2)—beryllium disks; (3)—Inconel gasket; and (4)—diamond anvils.



(a)



(b)

FIG. 2. (a) Miniature diamond anvil pressure cell mounted on standard x-ray goniometer head. (b) Pressure cell mounted on single crystal orienter of x-ray diffractometer.

by-point data acquisition in which each reflection is related to the entire reciprocal lattice by the Eulerian variables and 2θ .

DESIGN FEATURES

The main guidelines in the design of a new pressure cell was that it be small enough to mount on a standard goniometer head and meet the specifications of space requirements of a standard precession camera as well as the single crystal orienter. These features have been implemented by designing a highly simplified instrument in which the diamonds are placed on two small platens that are pulled together by three screws instead of the conventional method of pushing them together. In the construction of the platens, stainless steel was used in the shadow of the gasket as shown in Fig. 1. Beryllium¹² disks are used to support the diamonds and also serve as x-ray windows. These beryllium disks are 12.7 mm diam by 3.2 mm thick with a small axial hole 3.3 mm diam recessed 0.76 mm to position the diamonds. A second axial hole 1.0 mm diam is drilled through the disk for optical observation of the sample in the pressure chamber. The beryllium disks may be replaced by steel when only optical observations are being made. The assembled pressure cell is 32.0 mm diam by 15.9 mm. The x-ray beam can enter and exit in a cone of 50° half-angle which in specialized cases

permits the measurement of 2θ angles up to a maximum of 100° . If the total cell were constructed of beryllium similar to the NBS cell, it would be possible to measure reflections at higher cone half-angle but the shadowing of the gasket beyond approximately 55° make such intensity measurements unreliable unless appropriate corrections are made.¹³

The pressure cell is mounted on a standard goniometer head for which the only modification was the removal of the height adjustment mechanism. The single crystal orienter is designed so that the standard distance from the base of the goniometer head to the center of the sample chamber of the pressure cell cannot exceed 49 mm. In order to keep the arcs and translations of the goniometer head and conform to the height restriction, a flat surface was machined on the circumference of the pressure cell where the base is attached. This base assembly slides over the cylindrical sleeve from which the height adjustment mechanism was removed securing the pressure cell to the goniometer head. This assembly is secured by a set screw allowing vertical adjustment of the cell. This design allows one to take advantage of the translations and arcs plus a height adjustment for centering the sample in the x-ray beam. Most of the standard techniques for lineup of a single crystal can be used. The instrument requires no special accessories and can be mounted interchangeably on various single crystal x-ray diffraction devices (Fig. 2).

TECHNIQUES AND PROCEDURES

In this design there is no independent method of aligning the diamonds parallel to each other such as is found in the Bassett press or NBS press. In using a compressible gasket it is apparent that alignment is not critical at pressures up to 25 kilobars. Upon increasing pressure with a newly loaded sample, care is taken to uniformly tighten the three screws in small increments keeping the stainless steel platens as nearly parallel as possible. Very few gasket failures result when this procedure is followed. If the working range of the pressure cell were extended to higher pressures (i.e., 30–50 kilobar range), it is anticipated that better alignment of the diamonds would become more important.

An important problem encountered in the data collection using counting techniques is that of distinguishing between single crystal reflections originating from the sample and those originating from the diamonds. Satisfactory criteria for identifying the diamond reflections are (i) their much greater intensity and (ii) their 2θ positions. An additional criterion would be to determine the reciprocal lattice points for each of the diamonds but this has not been necessary yet. In the precession method the diamond spots can always be identified by their size and the streaks produced by white radiation. In the counting method, however, streaks introduce a serious problem. They sometimes extend over a 2θ range greater than 20° and their intensity is generally much greater than reflections from the sample. Two alternative methods for removing these streaks have been used. One method is to use a focusing presample monochromator while the second employs pulse height selection to discriminate against white radiation. The method selected for a particular

study depends upon the experimental requirements. For most studies, however, pulse height selection is adequate and by far the easier method. This is particularly true when a lattice has already been determined previously from precession photographs.

The focusing monochromator was used in collecting the intensity data for a study of the high pressure phases of calcium carbonate, $\text{CaCO}_3(\text{II})$ and $\text{CaCO}_3(\text{III})$. This method required some repositioning of the goniometer with respect to the x-ray tube. The monochromator used was a bent quartz crystal which was adjusted so as to focus the divergent beam emerging from the x-ray tube to a line at the sample. With this geometry, a fairly divergent scattered x-ray beam is observed at the detector as well as significantly improved intensities. The larger spot size made locating weak reflections much easier in the manual search. Experimentally the main disadvantage of the focusing monochromator as it is used here is its distortion of spot shapes in reciprocal space due to the divergence of the scattered beam. In the investigation of phenomena involving spot shapes, it would be necessary to rely on pulse height discrimination to reduce the white radiation streaks. The pulse height method could be improved significantly by the use of a solid-state detector. An important advantage of pulse height selection is that no modification of the diffraction geometry is required. The use of the monochromator with the precession camera proved to be of no advantage and was somewhat confusing due to the distorted shape of the spots on the film.

One of the advantages of using counting methods is the ability to detect and measure the intensities of very weak reflections. In the interpretation of such reflection it is important to recognize that the x-ray beam from a monochromator crystal is not completely monochromatic but contains an extra wavelength due to second order diffraction by the monochromator from the continuum. This may result in an extra set of weak reflections originating from the diamonds or the sample. Since the $\lambda_{K\alpha}/2$ x-ray intensity will be much weaker than the $\lambda_{K\alpha}$ intensity, these reflections can generally be identified by their 2θ position and appropriate intensity ratio to the $\lambda_{K\alpha}$ reflection.

The use of the high pressure cell to obtain meaningful intensity data for structure determination using counting methods was tested on the single crystal orienter using a calcite rhomb which was subjected to a pressure of about 5 kilobars. A total of 112 reflections were measured, 60 of which were independent. Two cycles of refinement of the positional parameter of oxygen gave a fit to the calcite structure in which the R index was 10%. The F values of equivalent reflections were averaged, however no correction was made for absorption through the beryllium or the diamonds. The absorption correction for this pressure cell ranges from 2% to 10% depending upon the angles which the incident and scattered x-ray beams make with the cell axis.

ANALYSIS OF ACCESSIBLE VOLUME

It is of interest to calculate the amount of reciprocal space that is available with this pressure cell. This can be carried out by considering all the orientations and magnitudes that

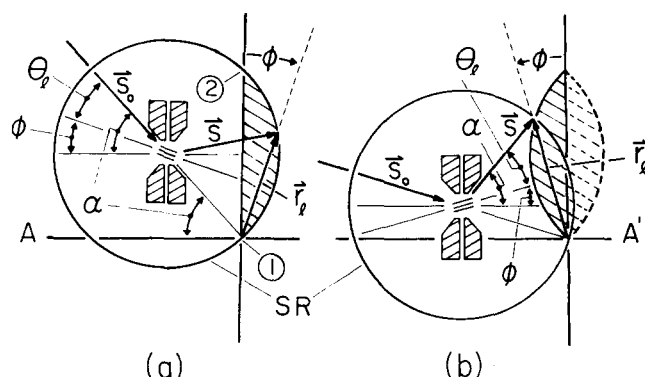


FIG. 3. Graphical relation of diffraction conditions, when using pressure cell, showing the limiting volume in reciprocal space in terms of the locus of the maximum values of the reciprocal lattice vector r_l . (SR) sphere of reflection. (a) When the normal to the crystal lattice planes makes an angle $(90 - \phi)$ with the cell axis, r_l traces the segment of the bounding curve between (1) and (2). For this condition the angles that S_0 and S make with the cell are (α) and $(\alpha - 2\phi)$, respectively. (b) When the normal to the crystal lattice planes makes an angle $(90 + \phi)$ with the cell axis, r_l traces the mirror image of arc 1-2 in (a). Note that the angles which S_0 and S make with the cell axis are reversed from their values in (a).

are possible for the reciprocal lattice vector to assume in view of the physical restrictions of the cell. Consider any crystal plane whose normal makes an angle $(90 - \phi)$ with the axis of the pressure cell as shown in Fig. 3(a). For a given value of ϕ , the limiting diffraction angle θ_l available is $(\alpha - \phi)$. Thus in reciprocal space the length of the limiting (maximum) reciprocal lattice vector is given by

$$r_l = [2 \sin(\alpha - \phi) / \lambda]. \quad (1)$$

It should be noted that the scattered x ray exits at an angle $(\alpha - 2\phi)$ to the cell axis. If other values of ϕ are selected in this same quadrant, corresponding values of r_l are determined, all of which fall on the reflection sphere representing solutions of the Laue equations. Since r_l are maximum values, that portion of the reflection sphere between (1) and (2) is the limit of reciprocal space accessible to the pressure cell. The other bounding curve is the mirror image of this arc as shown in Fig. 3(b). Points along this latter curve can be determined by considering crystal planes such that their normal makes an angle $(90 + \phi)$ with the cell axis. For given values of ϕ , corresponding values of r_l are determined which fall on this second arc. In this case, specification of the angle ϕ also specifies the angle of the incident x-ray beam as $(\alpha - 2\phi)$. The limits of reciprocal space accessible when using the pressure cell can now be illustrated by rotating the two arcs 360° about the AA' axis, generating a toroidal surface. It should be noted in foregoing illustrations [Figs. 3(a), (b)] that all the solutions of the Laue equations have not been investigated, but only those giving the maximum value of the reciprocal lattice vector.

The maximum volume V_m accessible in reciprocal space is determined by integration of Eq. (1) over the appropriate space coordinates, viz⁹

$$V_m = 2 \int_0^{2\pi} \int_0^\alpha \int_0^{r_l} r^2 \cos \phi dr d\phi d\omega. \quad (2)$$

By performing the integrations over dr and $d\omega$, and making

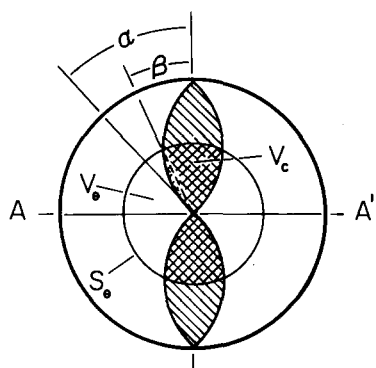


FIG. 4. Map of reciprocal space available to pressure cell and the relationship of the variables used to calculate the reciprocal volumes. The total accessible reciprocal volume V_m , is indicated by the total shaded region. (V_θ) total volume enclosed within full sphere S_θ with radius r_θ defined by practical diffraction angle limit 2θ , (V_c) volume accessible to pressure cell within the sphere S_θ is indicated by darker shading.

the substitution of variables $x = \alpha - \varphi$, then $-\cos x dx = \cos(\alpha - \varphi) d\varphi$ and V_m can be expressed as

$$V_m = \frac{32\pi}{3\lambda^3} \int_0^\alpha \sin^3 x \cos(\alpha - x) dx. \quad (3)$$

This expression is readily integrated by expanding $\cos(\alpha - x)$ in terms of its trigonometric identity giving

$$V_m = \frac{4\pi}{\lambda^3} \sin \alpha (\alpha - \sin \alpha \cos \alpha). \quad (4)$$

The accessible volume V_m is shown in Fig. 4 as the region enclosed by a toroidal surface whose cross sectional area is indicated by the shading. The bounding curves enclosing this shaded region are arcs of a circle whose radius is $1/\lambda$, the same as the radius of the reflection sphere. Equation (1) is the equation of this arc in the first quadrant. While Eq. (4) gives the total volume in reciprocal space accessible when using the pressure cell, it is more meaningful to compare the amount of reciprocal space in the region in which the actual data are obtained. Using Mo radiation, the number of

reflections necessary for a structure determination can generally be collected within the 2θ range of 40° – 60° . For comparison, we define a sphere S_θ which includes all of reciprocal space up to the practical limit of data collection, θ_m . The volume of this enclosed region is

$$V_\theta = \frac{32\pi}{3\lambda^3} \sin^3 \theta_m. \quad (5)$$

Of the volume of this sphere in reciprocal space, one is interested in that fraction which is accessible to the pressure cell. This fraction can be obtained by solving for the ratio V_c/V_θ where V_c is the accessible volume within S_θ (see Fig. 4). The accessible volume V_c can be evaluated in the same manner as Eq. (2) by breaking the integral into two parts and integrating over the appropriate limits (Fig. 4).

$$V_c = 2 \int_0^{2\pi} \int_0^\beta \int_0^{r_\theta} r^2 \cos \varphi dr d\varphi d\omega + 2 \int_0^{2\pi} \int_\beta^\alpha \int_0^{r_l} r^2 \cos \varphi dr d\varphi d\omega, \quad (6)$$

where

$$r_\theta = [2 \sin(\alpha - \beta)/\lambda], \quad (0 \leq \varphi \leq \beta), \quad (7)$$

giving the desired fraction

$$V_c/V_\theta = \frac{3}{4} \left[\sin(\alpha - \theta) + \frac{\sin \alpha}{2 \sin^3 \theta} (\theta - \sin \theta \cos \theta) \right], \quad (8)$$

where $(0 \leq \theta \leq \alpha)$.

These data are plotted in Fig. 5 for $\alpha = 40, 50$, and 60° . For the pressure cell described in this work ($\alpha = 50^\circ$), at the 2θ limits $40, 50$, and 60° , V_c/V_θ equals $58\%, 52\%$, and 46% , respectively.

Since V_c is the accessible volume in reciprocal space out to some practical 2θ limit in which the intensity data are collected, it is of interest to know what fraction this is of the total accessible reciprocal volume V_m . These data are plotted in Fig. 5 as V_c/V_m vs 2θ for the case $\alpha = 50^\circ$. Examination of this curve shows that at a 2θ limit of 60° , 55% of the total accessible volume V_m can be reached. The foregoing analysis applies to the use of a full circle goniometer or the precession method.

It should be noted that the important feature of data collection for a structure determination is not the total number of reflections but is the number of independent reflections that can be collected. In monoclinic $\text{CaCO}_3(\text{II})$ for example, there are 1680 lattice points in a full sphere of radius r_θ ($\theta = 25^\circ$) but only approximately 420 independent reflections. In this range, however, the total number of reflections accessible to the pressure cell ($\alpha = 50^\circ$) is 870, of which approximately 215 are independent. With crystals of higher symmetry, the number of independent reflections that can be collected in this range of 2θ will approach 100% due to the larger number of equivalent reflections present. In all crystal systems with the exception of cubic there is a possibility of lattice points along a unique axis or plane falling within an inaccessible region of reciprocal space due to the orientation of the crystal in the pressure cell. If the type

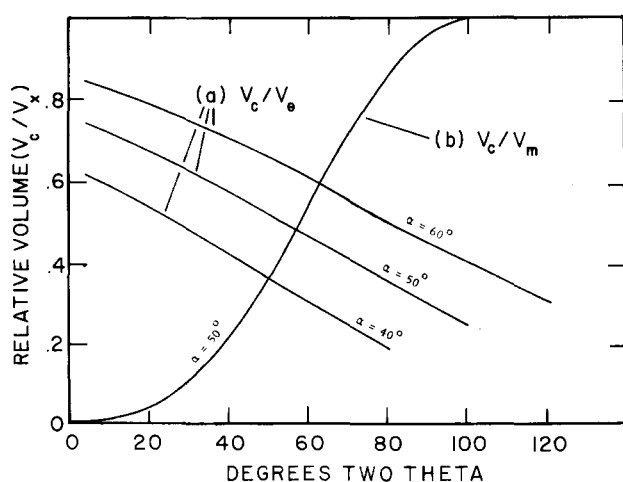


FIG. 5. (V_c/V_θ , $x = c, m$) (a) Ratio of V_c the accessible volume in S_θ to V_θ the total volume in S_θ . (b) Ratio of V_c the accessible volume in S_θ to V_m the maximum volume accessible to the pressure cell.

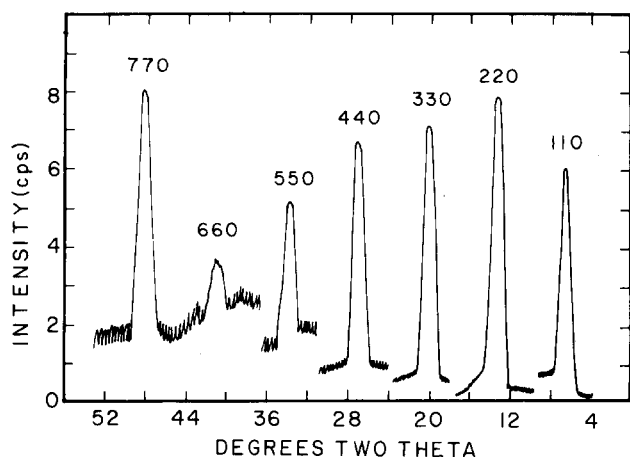


FIG. 6. Diffractometer trace of seven orders of the $h h 0$ reflections of $\text{CaCO}_3(\text{III})$ at an approximate pressure of 25 kilobars. The cps range and intensity of each reflection is given in Table I (note cps range applies to full scale value of 10).

of study permits, different orientations of the crystal can be used to collect data from these regions.

DISCUSSION

The principal advantages of this instrument lie in its simplicity and versatility. Experimentally the ability of the instrument to be used interchangeably on standard diffraction units allows one to combine the advantages of single crystal counting techniques with the precession method. Some of the advantages of counting techniques are the much improved signal to noise ratio and the ability to detect very weak reflections. These features are illustrated in Fig. 6 which is a 2θ scan showing seven orders of the $h h 0$ reflections of $\text{CaCO}_3(\text{III})$ at 25 kilobars. This trace was taken without a monochromator but with pulse height selection only. The scale and intensity of each reflection is given in Table I. In the counting method, the use of collimation and pulse height discrimination significantly reduce

TABLE I. Relative and integrated intensity for $h h 0$ reflections of $\text{CaCO}_3(\text{III})$ at a sample pressure of 25 kilobars.

$h h 0$	Scaler range (cps full scale)	Integrated intensity	Relative intensity
1 1 0	1000	1350	60
2 2 0	10 000	22 500	1000
3 3 0	2000	3500	160
4 4 0	500	820	40
5 5 0	200	150	7
6 6 0	100	35	1.5
7 7 0	100	140	6

background noise, while in the precession method the background is continually being recorded on the film and is enhanced by the additional scattering from the diamonds of the pressure cell. After the initial lineup of the sample and the determination of the space group symmetries by the precession method, the intensity measurements can be made with greater accuracy and ease with the single crystal orienter using counting methods. In summary, the simplicity, low cost, miniaturization, and the versatility of this instrument in fitting standard single crystal x-ray diffraction units is a significant improvement in the study of single crystal phases at high pressure.

ACKNOWLEDGMENTS

The authors wish to thank J. D. Barnett for suggesting the section entitled "Analysis of Accessible Volume" and for Eqs. (1)–(4). Thanks are also due R. L. Collin for use of his precession camera and x-ray generator. J. D. Barnett, R. L. Collin, and G. J. Piermarini have generously given help and constructive criticism in the writing of this paper. This work was supported by a grant from the National Science Foundation.

*Now at the High Pressure Data Center, Brigham Young University, Provo, Utah 84602

¹W. A. Bassett and T. Takahashi, *Am. Mineral.* **50**, 1576 (1965).

²W. A. Bassett, T. Takahashi, and P. W. Stook, *Rev. Sci. Instrum.* **38**, 37 (1967).

³C. E. Weir, S. Block, and G. J. Piermarini, *J. Chem. Phys.* **53**, 4265 (1970).

⁴C. E. Weir, S. Block, and G. J. Piermarini, *J. Res. Natl. Bur. Stand. (U.S.) C* **69C**, 279 (1965).

⁵D. Andre, R. Fourme, and M. Renaud, *Acta Crystallogr. B* **B27**, 2371 (1971).

⁶Y. K. Chang, "Diamond Synthesis," M. S. thesis, University of Rochester.

⁷J. R. Ferraro, "High Pressure Vibrational Spectroscopy," in *Spectroscopy in Inorganic Chemistry* (Academic, New York, 1971), Vol. 2, pp. 57–77.

⁸A. Van Valkenburg, "Visual Observations of Single Crystal Transitions under True Hydrostatic Pressures up to 40 kilobar," in *Conference Internationale sur-les-Hautes Pressions* (Le Creusot, Saone-et-Loire, France, 1965).

⁹C. E. Weir, E. R. Lippincott, A. Van Valkenburg, and E. N. Bunting, *J. Res. Natl. Bur. Stand. (U.S.) A* **63A**, 55 (1959).

¹⁰C. E. Weir, G. J. Piermarini, and S. Block, *Rev. Sci. Instrum.* **40**, 1133 (1969).

¹¹R. Fourme, *J. Appl. Crystallogr.* **1**, 23 (1968).

¹²Due to the extreme toxicity of beryllium, it is recommended that all machining of beryllium parts be done by the supplier.

¹³A. Santoro, C. E. Weir, S. Block, and G. J. Piermarini, *J. Appl. Crystallogr.* **1**, 101 (1968).

¹⁴J. D. Barnett, private communication.